Sonbul, Sultan N. and Gorringe, Kylie L. and Aleskandarany, Mohammed A. and Mukherjee, Abhik and Green, Andrew R. and Ellis, Ian O. and Rakha, Emad A. (2017) Chemokine (C-C motif) receptor 7 (CCR7) associates with the tumour immune microenvironment but not progression in invasive breast carcinoma. Journal of Pathology, 3 (2). pp. 105-114. ISSN 1096-9896

The Journal of Pathology: Clinical Research
J Path: Clin Res April 2017; **3:** 105–114
Published online 28 January 2017 in Wiley Online Library (wileyonlinelibrary.com). DOI: 10.1002/cjp2.65

Original Article

Chemokine (C-C motif) receptor 7 (CCR7) associates with the tumour immune microenvironment but not progression in invasive breast carcinoma

Sultan N Sonbul,[1,2] Kylie L Gorringe,[3] Mohammed A Aleskandarany,[1] Abhik Mukherjee,[1] Andrew R Green,[1] Ian O Ellis[1] and Emad A Rakha[1]*

[1] *Division of Cancer and Stem Cells, School of Medicine, The University of Nottingham, and Nottingham City Hospital, Nottingham University Hospitals NHS Trust, Nottingham, UK*
[2] *Biochemistry Department, Faculty of Sciences, King Abdulaziz University, Jeddah, Kingdom of Saudi Arabia*
[3] *Cancer Genomics Program, Peter MacCallum Cancer Centre, Melbourne, and The Sir Peter MacCallum Department of Oncology, University of Melbourne, Parkville, Australia*

*Correspondence to: Emad A Rakha, Division of Cancer and Stem Cells, School of Medicine, The University of Nottingham, and Nottingham City Hospital, Nottingham University Hospitals NHS Trust, Hucknall Road, Nottingham NG5 IPB, UK. E-mail: emad.rakha@nottingham.ac.uk

Abstract

Some previous studies have reported that the chemokine (C-C motif) receptor 7 (CCR7) plays a role in breast cancer, is associated with lymph node metastasis and drives the site of distant metastasis. However, the impact of its expression on patient outcome and its association with tumour infiltrating inflammatory cells remain to be validated. We evaluated CCR7 protein expression by immunohistochemistry in a large well characterized cohort ($n = 866$) of early invasive primary breast cancers. CCR7 was expressed in the cytoplasm and membrane of tumour cells. We observed a weak positive association of high CCR7 expression when in either cellular component, but not both together, with axillary lymph node stage 3 tumours ($p = 0.043$). Logistic regression analysis of lymph node stage revealed no independent predictive value for CCR7 expression. CCR7 expression was higher in HER2 positive tumours ($p = 0.03$) and associated with positive CD68+ FOXP3+ tumour infiltrating cells. CCR7 staining was negatively associated with CD3+ cells. There was no significant association of CCR7 expression with breast cancer recurrence or survival. We conclude that while CCR7 is not a useful biomarker for predicting lymph node metastasis, it may reflect altered intra- and inter-cellular signalling related to the immune microenvironment. The subcellular localization of CCR7 appears to affect the nature of these interactions.

Keywords: immune response; cancer microenvironment; metastasis; breast cancer; immunohistochemistry

Received 11 November 2016; Accepted 22 January 2017

No conflicts of interest were declared.

Introduction

Invasive breast cancer (IBC) has increasingly good survival rates, but once metastatic disease is present, survival rates decline sharply even in subtypes with generally good prognosis. Determinants of metastasis are many and varied; however, the interaction of the tumour with the surrounding microenvironment is a key factor that includes the activation of tumour cell chemotaxis through specific chemoattractants in a cell–cell or cell–matrix crosstalk. These biological interactions are regulated in a cluster of convergent and meticulous signalling, transcriptional, translational and post-translational pathways [1].

Previous studies reported that the targeted migration of IBC cells toward lymphatics is stimulated by tumour cell expression of chemokine (C-C motif) receptor 7 (CCR7) which binds to its ligands, the lymphoid-homing chemokines CCL19/CCL21 [2,3]. CCR7 is a protein with G-protein coupled receptor activity that biologically functions in cellular polarity, motility, and chemotaxis [4]. The expression of CCR7 by IBC cells has been reported to promote growth, proliferation, and metastasis of breast cancer cells in animal models [5]. CCR7 expression has been reported to correlate with vascular endothelial growth factor C and the lymphatic endothelial marker podoplanin [6]. Moreover, proliferation of blood and

lymphatic endothelial cells through angiogenesis and lymphangiogenesis pathways has been attributed to actions mediated by CCR7 [6,7].

A number of studies in breast cancer cohorts have shown that both mRNA and protein expression of CCR7 are higher or more frequently expressed in tumours with lymph node metastasis [8–12]. In contrast, analysis of the METABRIC expression data found that this association was limited to the Luminal B subtype (oestrogen receptor (ER) positive, high proliferation group) [13]. Another study suggested that COX2 expression was required for this association to be significant [14]. Association of CCR7 with distant metastatic sites has varied from skin [8] to bone [15] to none [16]. These dissenting studies may suggest that inter-cohort heterogeneity with respect to tumour subtypes may be the reason for the lack of a consistent association of CCR7 expression with disease-free or breast-cancer specific survival. To date, only a single report of an association of protein expression with worse overall survival has been found [11], with other studies showing at best weak trends [8,16–18].

In this study, we aimed to resolve the association of CCR7 with site of metastasis and patients' breast cancer specific survival in a large cohort of early IBC patients with extensive clinical and molecular characterization.

Materials and methods

Study cohort

The specimens in this study were derived from the well-characterized Nottingham Tenovus Primary Breast Carcinoma Series and consisted of 866 unselected primary operable IBC female patients. The detailed clinico-pathological profiles of the patients included histological phenotype, molecular subtypes, primary tumour size, histological grade, tumour stage, nodal status, distant metastasis, lymphovascular invasion and Nottingham Prognostic Index (Table 1) [19]. Disease-free survival and breast cancer specific survival have been recorded for up to 25 years (median 175 months, range 1–305 months) and include information on local and regional recurrences, distant metastasis and disease specific mortality. Immunohistochemistry data for a broad panel of biomarkers is available for this cohort including ER, HER2, Ki67, pAKT and immune-related markers including CD68, CD3, CD8 and FOXP3 as previously published [20–23].

Table 1. Clinico-pathologicial characteristics of the cohort ($n = 866$)

Feature	N	%
Age		
≤ 50 years	303	35.0
> 50 years	563	65.0
Tumour size		
≤ 20 mm	413	47.7
> 20 mm	453	52.3
Grade		
1	130	15.0
2	298	34.5
3	436	50.5
Stage		
1	538	62.1
2	255	29.4
3	71	8.2
Tumour type		
Ductal no special type	738	85.2
Classical Lobular	74	8.5
Medullary-like	20	2.3
Tubular/Mucinous	22	2.5
Others	12	1.4
ER status		
Negative	211	24.4
Positive	651	75.2
Not available	4	0.5
HER2 status		
Negative	720	83.1
Positive	122	14.1
Not available	24	2.8
IHC subtype		
HER2 (ER−, HER2+)	58	6.7
LUMA (ER+, Ki67 low, HER2−)	203	23.4
LUMB (ER+, Ki67 high or HER2+)	348	40.1
NEG (ER−, HER2−)	144	16.6
ER+ no Ki67 data	102	11.7
ER+, Ki67 high, HER2-	280	32.2
Any HER2+	121	13.9
Not available	13	1.5

All experiments were conducted in compliance with the current ethical and legal guidelines of the United Kingdom. Ethics approval was obtained from the Nottingham Research Ethics Committee and this study is in accordance with the 1975 Helsinki declaration and its later amendments or comparable ethical standards.

Western blot analysis

Western blot was performed to assess the binding specificity of rabbit monoclonal anti-CCR7 antibody [(Y59), ab32527, Abcam, UK] to its target, residues in the N-terminal extracellular domain. In brief, four breast cancer cell lysates, MCF7, MDA-MB-231, MDA-MB-468, SKBR3, together with lysates from MCF10A (normal breast epithelial) and HeLa cells were electrophoresed though a NuPAGE Bis-Tris Mini Gel 4–12% (Invitrogen, UK) with MOPS SDS

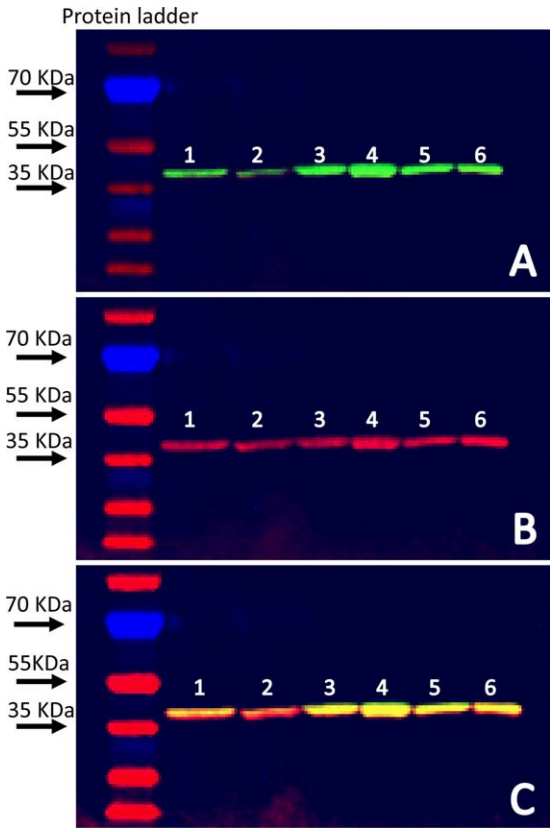

Figure 1. Validation of the anti-CCR7 antibody. Western blotting showing specific antigen-binding of the anti-CCR7 primary antibody in the cell line lysates of: MCF7, lane 1, SKBR3, lane 2, MDA-MB-231, lane 3, MDA-MB-468, lane 4, HeLa, lane 5 and MCF10A, lane 6. (A) CCR7 protein at the expected molecular weight of 42.87 kDa, visualized in lanes 1–6 as green fluorescent bands in the 800 channel of the Odyssey Imaging System. (B) β-actin protein at the expected molecular weight of 42 kDa visualized in lanes 1–6 as red fluorescent bands in the 700 channel of Odyssey Imaging System. (C) Multiplexed image of both anti-rabbit and anti-mouse secondary antibodies used in (A) and (B). The yellow bands indicate the overlapping proteins with molecular weight around 42 kDa. The molecular weight marker has both red and blue colored bands.

Running Buffer (Invitrogen, UK), and drops of anti-oxidant reagent, NuPAGE Anti-Oxidant (Invitrogen, UK) for 90 min at 150 V. Following transfer to the membrane for 60 min at 30 V, 5% of Marvel Milk in washing buffer PBS-Tween 20 (0.1%) was used as the blocking buffer for 60 min.

Anti-CCR7 antibody was applied at 1:5000 in blocking buffer; mouse monoclonal anti-βactin primary antibody was used as a marker of endogenously expressed control. The primary antibody was incubated for 12 h. Fluorescent secondary antibodies, anti-rabbit and anti-mouse (Odyssey, Lot#C20926-02, Lot#C20919-01) were used at 1:2000. The multiplexed images of the detected bands were visualized using the infrared imaging system of Li-Cor Biosciences, Odyssey (Figure 1).

Immunohistochemistry

The immunostaining procedure was performed using Novocastra Novolink^{TM} Polymer Detection Systems kit (Code: RE7280-K, Leica, Biosystems, UK) on 4 µm thick formalin fixed paraffin-embedded of full-face ($n = 15$) and tissue microarray (TMA) sections. Sections were incubated for 1 hour with the anti-CCR7 antibody [(Y59), ab32527, Abcam, UK] diluted at 1:5000 using Bond Primary Antibody Diluent (Ref#AR9352, Leica, Biosystems, UK). The bound anti-CCR7 antibody was chemically chained with Novolink^{TM} Polymer, anti-rabbit Poly-HRP-IgG [<25 μg/mL] containing 10% [v/v] animal serum in tris-buffered saline (0.09%) ProClin^{TM} 950, for 30 min. Finally, DAB chromogen reagent, 1.74% w/v 3,3′-diaminobenzidine, in a stabilizer solution, was added for 5 min, and followed by the addition of 0.1% Haematoxylin as a counter stain.

Scoring of CCR7 expression

High resolution digital images (Nanozoomer; Hamamatsu Photonics, Welwyn Garden City, UK) scanned at $\times 20$ magnification were used to facilitate scoring of the TMA cores using the NDP.view2 software (Hamamatsu Photonics, Systems Division). Four different staining intensities for CCR7 (0, 1, 2 and 3) were given for the invasive cancer cells within the evaluated TMA cores (Figure 2). The expression of CCR7 was assessed semi-quantitatively using the histo-score (H-score) method. Staining intensity was multiplied by the percentage of representative cells in the tissue for each intensity, producing a range of values between 0 and 300 [24]. Two independent observers (Sonbul S and Mukherjee A) performed the assessment, and major discrepancies were rescored by both scorers using a double-headed microscope. The cut-off point, for either cytoplasmic or membranous expression, used was chosen based on the median H-score: negative/low ≤ 120 and positive >120 H-score. A summed H-score was used to evaluate total CCR7 expression, with a threshold of 240.

Statistical analysis

Cohen's kappa coefficient of agreement tests was used as appropriate with a value below 0.75 considered to be a weak agreement between the scores of both observers. Chi-square was used in the analysis of the categorical CCR7 levels in relationship to

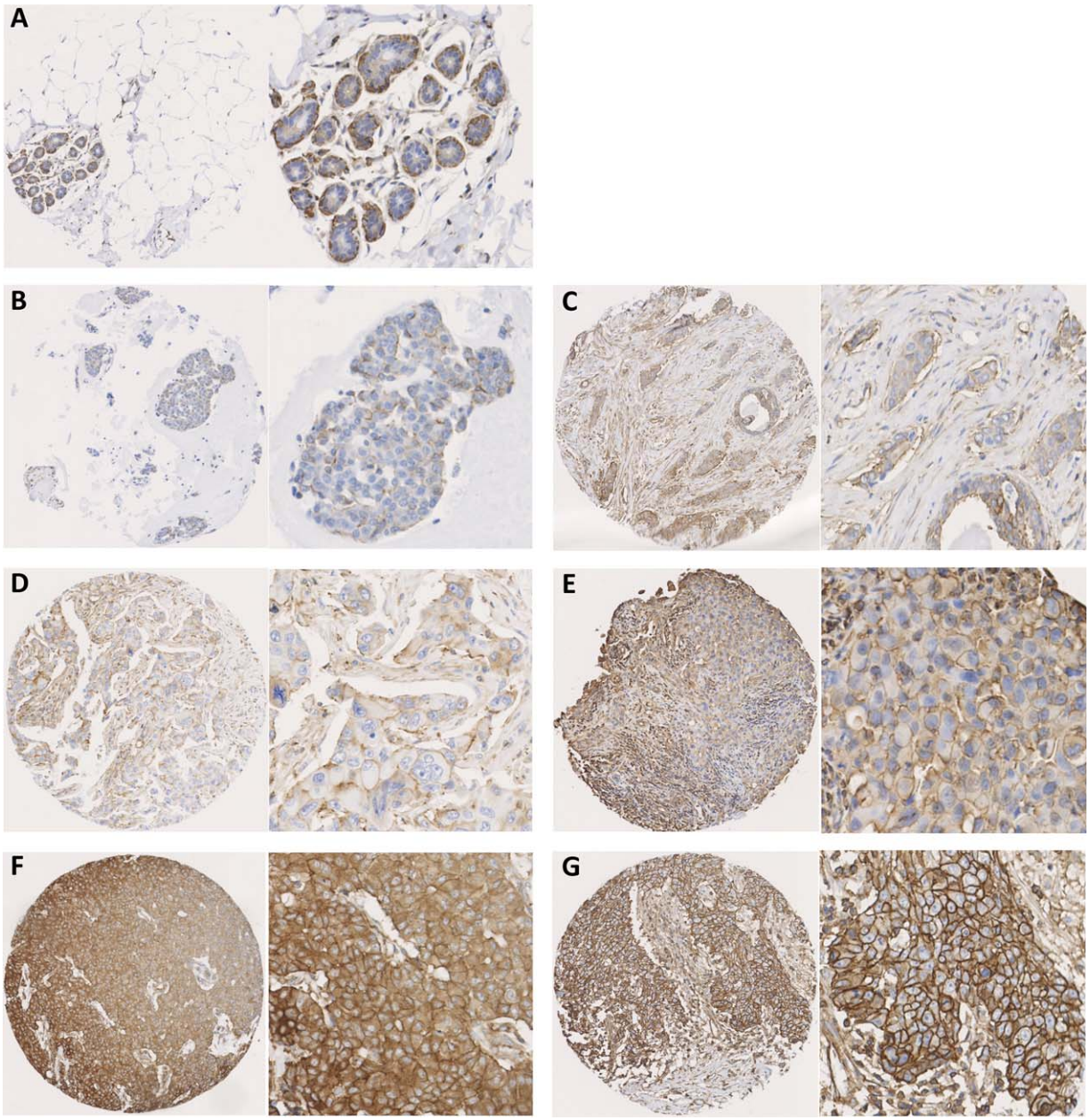

Figure 2. Immunohistochemical staining patterns of CCR7 in normal and malignant breast tissue. Immunostaining of TMA slides showing subcellular localization of CCR7 with cytoplasmic and membranous expression: (A) normal breast terminal duct lobular units. Invasive breast cancer with: (B) negative cytoplasmic expression, (C) negative membrane expression, (D) low cytoplasmic expression, (E) low membrane expression, (F) positive cytoplasmic expression, (G) positive membrane expression. Objective magnifications are ×10 (left) and ×20 (right).

clinical and molecular variables. For all tests, a two-tailed P value of <0.05 was considered as significant. Analyses were performed using SPSS (Chicago, IL, USA). Logistic regression and survival analyses were performed in R using glm, stepAIC (stepwise Akaike Information Criterion model selection) and coxph. CCR7 was considered as both a categorical variable using the median threshold above, and also by the continuous H-score data.

Results and discussion

Immunohistochemistry and clinico-pathological associations

Evaluation of the CCR7 antibody using Western analysis showed highly specific detection of the protein at the expected size of 42.87 kDa (Figure 1). In the tumour-associated normal epithelial breast cells,

Table 2. Statistical associations of CCR7 cytoplasmic expression with clinico-pathological parameters

	Negative/Low CCR7		Positive CCR7			
Parameter	*N*	(%)	*N*	(%)	χ^2	*P* value
Age (years)						
≤ 50	145	31.6	158	38.8	4.96	**0.026**
> 50	314	68.4	249	61.2		
Size (mm)						
≤ 20	207	45.1	206	50.6	2.63	0.105
> 20	252	54.9	201	49.4		
Axillary nodal stage						
1	283	61.8	255	62.8	2.60	0.273
2	131	28.6	124	30.5		
3	44	9.6	27	6.7		
Grade						
1	69	15.1	61	15.0	1.865	0.394
2	167	36.5	131	32.3		
3	222	48.5	214	57.7		
Distant metastasis						
Yes	174	38.2	253	37.4	0.056	0.813
No	282	61.8	151	62.6		
Tumour histological type						
Invasive Ductal NST	384	83.7	354	87.0	3.89	0.42
Lobular	45	9.8	29	7.1		
Medullary-like	13	2.8	7	1.7		
Tubular/mucinous	12	2.6	10	2.5		
Others	5	1.1	7	1.7		
IHC subtype						
HER2 (ER−, HER2+)	25	6.2	33	9.5	3.17	0.37
LumA (ER+, Ki67 Low)	112	27.7	91	26.1		
LumB (ER+, KI67 High or HER2+)	187	46.2	161	46.3		
Negative (ER−, HER2−)	81	20.0	63	18.1		
HER2 status						
HER2+ (ER+ or ER−)	51	11.4	71	18	7.844	**0.009**
HER2− (ER+ or ER−)	397	88.6	324	82.0		

Values in bold represent values below the threshold of statistical significance; 0.05.

moderate cytoplasmic staining was observed. Staining of full-face sections in 15 IBC cases revealed homogenous expression of CCR7 when present (supplementary material, Figure S1); hence, the applicability of using TMAs was validated. In the malignant cells, CCR7 staining was observed as membranous and cytoplasmic staining and each was scored independently. No nuclear staining was observed. In these 15 cases a very few tumour infiltrating lymphocytes (<1%) with moderate to weak CCR7 expression were observed (supplementary material, Figure S1).

Positive cytoplasmic expression of CCR7 (H-score >120) was observed in 407/866 (47%) of tumours, and only 27/866 (3%) were entirely negative. In contrast, 99/866 tumours (11%) were negative for membrane staining and 410/866 (47%) positive (H-score > 120). There was a positive correlation between cytoplasmic and membrane staining ($r^2 = 0.38$, $p < 0.001$, Pearson correlation). 40% of cases had low or negative staining for both compartments, 13% had positive cytoplasmic staining only, 13% had positive membrane staining only and the remaining 34% had positive staining in both.

Few statistically significant associations were observed between CCR7 protein levels and clinico-pathological features for total staining, cytoplasmic staining, membrane staining or the combination of both (Tables 2–4; supplementary material, Table S1). High cytoplasmic staining was associated with younger patient age at presentation ($p = 0.026$), while low staining in both compartments was associated with lower tumour grade ($p = 0.026$).

Surprisingly, there was no association between CCR7 expression and axillary nodal stage even when binarized into lymph node positive and negative cases. Given this contrast with the literature, we evaluated whether our threshold selection may have influenced the results. The distribution of H-scores between lymph node negative (stage 1) and lymph node positive (stage 2 and 3) cases was not different (Figure 3, $p = 0.93$ and $p = 0.82$, Kolmogorov–Smirnov test for cytoplasmic and membrane CCR7

Table 3. Statistical associations of CCR7 membrane expression with clinico-pathological parameters

	Negative/Low CCR7		Positive CCR7			
Parameter	*N*	(%)	*N*	(%)	χ^2	*P* value
Age (years)						
≤ 50	150	32.9	153	37.3	1.856	0.17
> 50	306	67.1	257	62.7		
Size (mm)						
≤ 20	216	47.4	197	48.0	0.04	0.84
> 20	240	52.6	213	52.0		
Axillary nodal stage						
1	282	62.0	256	62.6	2.921	0.23
2	129	28.4	126	30.8		
3	44	9.7	27	6.6		
Grade						
1	79	17.4	51	12.5	4.682	0.096
2	258	34.7	140	43.2		
3	218	47.9	218	53.3		
Distant metastasis						
Yes	171	37.7	154	37.8	0.001	0.98
No	282	62.3	253	62.2		
Tumour histological type						
Invasive ductal NST	386	84.6	352	85.9	2.57	0.63
Lobular	37	8.1	37	9.0		
Medullary-like	11	2.4	9	2.2		
Tubular/mucinous	15	3.3	7	1.7		
Others	7	1.5	5	1.2		
IHC subtype						
HER2 (ER−, HER2+)	27	6.7	31	8.8	5.136	0.16
LumA (ER+, Ki67 Low)	121	30.1	82	23.4		
LumB (ER+, KI67 High or HER2+)	177	44.0	171	48.7		
Negative (ER−, HER2−)	77	19.2	67	19.1		
HER2 status						
HER2+ (ER+ or ER−)	56	12.6	66	16.6	2.49	0.115
HER2− (ER+ or ER−)	390	87.4	331	83.4		

respectively) suggesting that selection of the median H-score as a cut-off point was not the cause. Interestingly, when we looked at the association of CCR7 with nodal stage by cellular compartment, we found that either membrane or cytoplasmic, but not both together, were associated with stage 3 cases only ($p = 0.043$). While 39% of stage 3 cases were positive for either and 18% positive for both, only 23% of stage 1 cases were positive for either but 35% for both. CCR7 was not different in stage 2 cases (Figure 3). In terms of metastatic site, there were trends for lower cytoplasmic expression in cases with bone metastases ($p = 0.06$) and for higher membrane staining in cases with liver metastases ($p = 0.06$). Thus, high CCR7 was only associated with advanced breast cancer lymph node metastases (more than three nodes affected) and only when the CCR7 was located in a singular compartment. Indeed, the presence of CCR7 in both sub-cellular compartments was not associated with metastatic spread.

We subsequently performed logistic regression analysis to evaluate whether CCR7 would predict lymph node status, given other confounding features such as grade, tumour size, ER status, HER2 status and/or tumour molecular subtype. Only grade and tumour size were consistently included as significant factors in the model; CCR7 staining was not significantly independent, regardless of which sub-cellular component was considered.

We then investigated whether tumour molecular subtype could be related to CCR7 staining using the St Gallen recommendations for estimating intrinsic subtype based on IHC of ER, HER2 and Ki67 (in which Luminal B includes HER2 positive cases, [25]). Using this system, no association of CCR7 staining and subtype was identified (Tables (2–4)). However, when HER2 positive cases were considered as a separate group, there was some significant enrichment in higher staining for CCR7 [Tables 2, 4; $p = 0.009$ (cytoplasmic), $p = 0.03$ (both membrane and cytoplasmic), HER2+ vs. all others]. This association may be related to the location of CCR7 near the HER2 amplicon on 17q and is consistent with mRNA analysis in the METABRIC cohort [13]. When subgroup analysis of axillary lymph node stage was performed, CCR7 combined staining was significantly associated with

Table 4. Statistical associations of combined CCR7 cytoplasmic and membrane expression with clinico-pathological parameters

Parameter	Both low	Memb high	Cyto high	Both high	χ^2	*P* value
Age (years)						
≤ 50	112	33	38	120	6.277	0.099
> 50	235	79	71	178		
Size (mm)						
≤ 20	161	46	55	151	3.596	0.31
> 20	186	66	54	147		
Axillary nodal stage						
1	220	63	62	193	12.993	**0.043**
2	96	35	33	91		
3	30	14	14	13		
Grade						
1	62	7	17	44	14.37	**0.026**
2	128	39	30	101		
3	156	66	62	152		
Distant metastasis						
Yes	125	49	46	105	3.998	0.26
No	220	62	62	191		
Histological tumour type						
Invasive ductal NST	292	92	94	260	10.23	0.60
Lobular	32	13	5	24		
Medullary-like	9	4	2	5		
Tubular/mucinous	10	2	5	5		
Others	4	1	3	4		
IHC subtype						
HER2 (ER−, HER2+)	17	8	10	23	11.46	0.25
LumA (ER+, Ki67 Low)	95	17	26	65		
LumB (ER+, KI67 High or HER2+)	113	54	44	117		
Negative (ER−, HER2−)	61	20	16	47		
HER2 status						
HER2+ (ER+ or ER−)	35	16	21	50	8.803	**0.032**
HER2− (ER+ or ER−)	303	94	87	237		

Values in bold represent *P* values below the threshold of the statistical significance; 0.05.

stage in Luminal A ($p = 0.008$) and Luminal B ($p = 0.009$) cases, and also HER2 negative cases (ER− and ER+, $p = 0.01$). Each group reflected the same pattern as seen for all subtypes together. Membrane staining alone was inversely significantly associated with stage within the Luminal B tumours only ($p = 0.008$). This result contrasts with an analysis of the METABRIC study data, where the only significant association of lymph node status and CCR7 mRNA expression was a positive correlation in the Luminal B subtype [13]. However, in the subset of cases for which we have both mRNA and IHC data ($n = 144$, as part of the METABRIC study), mRNA and protein H-score did not correlate (Spearman $r < 0.02$ for all compartments).

Our data indicate that CCR7 is more often highly expressed in HER2 positive tumours, and also that low expression of CCR7 in both compartments is weakly associated with low grade. Additionally, in our unselected cohort, both HER2 positivity and high grade were positively correlated with axillary lymph node positivity ($p = 0.03$ and $p < 0.001$, respectively). Consequently, it is possible that previously observed strong associations of CCR7 with lymph node status may be due to selection of cases with a biased proportion of HER2 positivity or high grade in the lymph node positive cases. Indeed, of the four previous IHC studies of CCR7, two selected even numbers of lymph node positive and lymph node negative cases without matching for molecular subtype or tumour grade [9,11], a third used a small unselected set but did not provide either grade or HER2 data [10], and a final study did not observe any CCR7 staining in tumour epithelial cells [18]. The largest of these studies had just over 200 cases, which is insufficient for subgroup analysis, unlike our cohort.

Association of CCR7 localization and cell signalling interactions

The subcellular localization of CCR7 is critical to its function. In several different immune cell types CCR7 is primarily localized to the plasma membrane as a G-protein coupled receptor. After ligand stimulation with CCL19 or CCL21 it undergoes endocytosis,

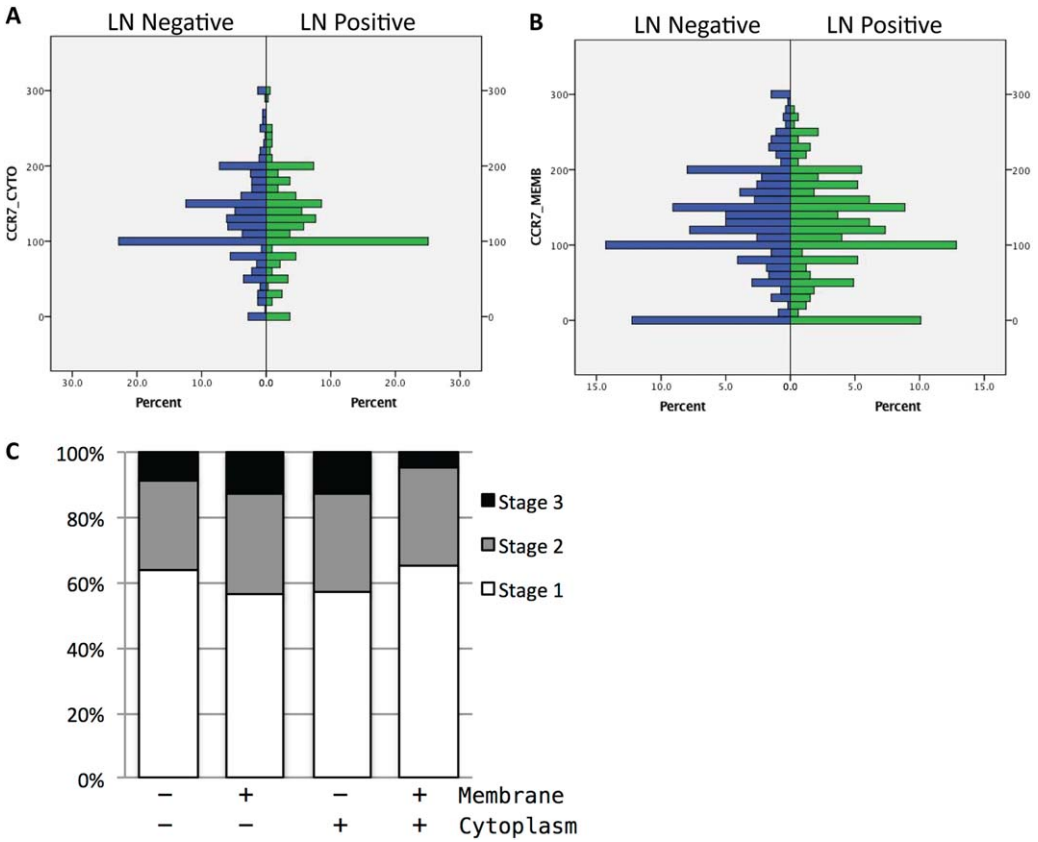

Figure 3. CCR7 expression is not related to lymph node status. Histogram of CCR7 (A) cytoplasmic and (B) membrane staining H-scores as a percentage of cases that are lymph node negative (blue) or lymph node positive (green). (C) Percentage of cases with high CCR7 staining across different cellular compartments (cytoplasmic, membrane or both) and association with axillary lymph node stage (1 = no positive nodes, 2 = 1–3 positive nodes, 3 = more than 3 positive nodes).

but is then recycled back to the membrane [26]. Membrane-associated CCR7 has been shown to be linked to an active chemotactic response, including to macrophages [27] and T lymphocytes. CCR7 positivity has previously been associated with high intra-tumoural FOXP3+ cells in gastric cancer, and both proteins were associated with lymph node metastasis and worse survival [28]. In this study, we also saw positive associations between high CCR7 membrane and also total CCR7 expression and the presence of FOXP3+ tumour infiltrating cells in the adjacent stroma ($p = 0.002$, $p = 0.004$ respectively) as well as a trend for higher intra-tumoural FOXP3+ cells ($p = 0.07$, $p = 0.05$). Intra-tumoural CD68+ cells were also present in higher numbers in tumours where CCR7 was highly expressed at the membrane ($p = 0.007$). CCR7 positivity was not associated with higher CD20+ or CD8+ cells. We previously showed that high numbers of CD68+ or FOXP3+ cells are associated with worse prognostic factors [21,22]. Although correlative, these data suggest an interaction between tumour membrane CCR7 expression and the recruitment of macrophages and T regulatory lymphocytes within the tumour microenvironment.

In contrast to membrane localization, cells with only cytoplasmic CCR7 do not respond to CCL19/CCL21 stimulation, and yet here and in other cancer types high CCR7 expression in the cytoplasm alone is often observed. It has been suggested that this type of expression may reflect a specific role for cytoplasmic CCR7 that is independent of a chemotactic interaction [29]. Cytoplasmic CCR7 staining and total CCR7 staining were inversely associated with the presence of CD3+ cells in the distant stroma ($p = 0.01$, $p = 0.006$ respectively), and this association was strengthened when considering only ER−HER2− tumours ($p = 0.006$). In this latter subgroup, 83% of CCR7 cytoplasm-low cases were CD3+ positive in the distant stroma, in contrast to 59% of CCR7 positive cases. In addition, all ER−HER2− cases with low total CD3+ counts were positive for CCR7 cytoplasmic staining. Thus, cases with CCR7 cytoplasmic staining may be enriched for a subgroup of ER−HER2− with a low T-lymphocyte response.

For cells with both high membrane and cytoplasmic CCR7 staining, we observed a counter-intuitive negative association with axillary nodal stage 3 cases. Other studies in different cancer types have not to date separated cases by subcellular localization of CCR7 staining. Therefore, it is unclear what such high expression in multiple cellular components may mean functionally for a tumour cell. We speculate that such staining may in some cases indicate an aberrant pattern whereby the usual trafficking of CCR7 between the membrane and the cytoplasm has been compromised. In HEK293 cells, expression of a CCR7 cDNA lacking lysine residues critical for ubiquitylation delayed recycling of the protein from endosomes back to membrane after ligand stimulation. CCR7 protein was observed to accumulate in the Golgi network, and this impaired recycling led to a defect in migratory chemokine response [30]. Such abnormal trafficking may represent a cellular context that does not provide a selective advantage for lymph node metastasis. This hypothesis could be tested by performing a similar CCR7 over expression experiment in breast cancer cells both *in vitro* (assessing chemokine response) and *in vivo* (evaluating metastatic potential).

Survival analysis

In order to assess any effect of CCR7 on patient survival, we performed Akaike Information Criterion analysis using axillary nodal stage, tumour grade, tumour size, ER status and HER2 status as factors in the model along with the CCR7 H-score. In both disease-free and breast-cancer specific survival, CCR7 membrane staining or a combined H-score summing cytoplasmic and membrane staining were included in the final models, as was CCR7 cytoplasmic staining for disease-free survival (see supplementary text). Similar results were obtained when CCR7 staining was input as a categorical variable. These results suggested that CCR7 protein expression added independent prognostic information to the survival model. However, when the Cox regression output was examined, this contribution was not significant at a $p < 0.05$ level, indicating that the effect of CCR7 protein expression is small and dependent on other factors. This borderline association of CCR7 with survival suggests that the previous conflicting studies would have been likely influenced by sample selection, nudging the results into significance in certain small cohorts.

In conclusion, we do not find strong evidence to suggest that CCR7 protein is a useful biomarker of lymph node metastasis, disease free recurrence or breast-cancer specific survival. However, we do find a link with high axillary node stage and specific subcellular localization of CCR7. While there was a correlation between CCR7 and HER2 positivity, the molecular subtype analyses enabled by our large cohort did not find any significant associations with survival when performed within subgroups. However, CCR7 was associated with altered tumour microenvironment, which may influence tumour capacity to spread through the lymphatic system. The association depends upon the subcellular localization of CCR7, with membrane staining showing an association with the presence of macrophages and regulatory T cells, whereas cytoplasmic staining was associated with CD3+ T cells. These associations require functional validation, for example by exogenous expression of various mutated forms of CCR7, with defective membrane or cytoplasmic localization, in an immune competent mouse model system of breast cancer to evaluate the impact on the tumour immune microenvironment. The distinct roles of CCR7 at the membrane and the cytoplasm deserve further attention, particularly in a cancer context.

Acknowledgements

Cell lysates were obtained from Prof. Stewart Martin (Faculty of Medicine & Health Sciences, The University of Nottingham). We thank Nottingham Health Science Biobank and Breast Cancer Now for their support with tissue TMA construction. KLG was supported by a UICC Yamagiwa-Yoshida Memorial International Cancer Study Grant.

Author contributions

EAR, ARG, IOE conceived of the study, contributed to study design and provided samples; SNS, AMA, AM, ARG collected data; SNS carried out experiments; KLG and SNS analysed and interpreted data and generated the figures; all authors contributed to drafting and reviewing the manuscript and approved the submitted and published versions.

References

1. Pang MF, Georgoudaki AM, Lambut L, *et al*. TGF-beta1-induced EMT promotes targeted migration of breast cancer cells through the lymphatic system by the activation of CCR7/CCL21-mediated chemotaxis. *Oncogene* 2016; **35:** 748–760.
2. Haessler U, Teo JC, Foretay D, *et al*. Migration dynamics of breast cancer cells in a tunable 3D interstitial flow chamber. *Integr Biol (Camb)* 2012; **4:** 401–409.
3. Muller A, Homey B, Soto H, *et al*. Involvement of chemokine receptors in breast cancer metastasis. *Nature* 2001; **410:** 50–56.

4. Hornbeck PV, Zhang B, Murray B, *et al*. PhosphoSitePlus, 2014: mutations, PTMs and recalibrations. *Nucleic Acids Res* 2015; **43:** D512–D520.
5. Cunningham HD, Shannon LA, Calloway PA, *et al*. Expression of the C-C chemokine receptor 7 mediates metastasis of breast cancer to the lymph nodes in mice. *Transl Oncol* 2010; **3:** 354–361.
6. Tutunea-Fatan E, Majumder M, Xin X, *et al*. The role of CCL21/CCR7 chemokine axis in breast cancer-induced lymphangiogenesis. *Mol Cancer* 2015; **14:** 35.
7. Chi BJ, Du CL, Fu YF, *et al*. Silencing of CCR7 inhibits the growth, invasion and migration of prostate cancer cells induced by VEGFC. *Int J Clin Exp Pathol* 2015; **8:** 12533–12540.
8. Andre F, Cabioglu N, Assi H, *et al*. Expression of chemokine receptors predicts the site of metastatic relapse in patients with axillary node positive primary breast cancer. *Ann Oncol* 2006; **17:** 945–951.
9. Cabioglu N, Yazici MS, Arun B, *et al*. CCR7 and CXCR4 as novel biomarkers predicting axillary lymph node metastasis in T1 breast cancer. *Clin Cancer Res* 2005; **11:** 5686–5693.
10. Li F, Zou Z, Suo N, *et al*. CCL21/CCR7 axis activating chemotaxis accompanied with epithelial-mesenchymal transition in human breast carcinoma. *Med Oncol* 2014; **31:** 180.
11. Liu Y, Ji R, Li J, *et al*. Correlation effect of EGFR and CXCR4 and CCR7 chemokine receptors in predicting breast cancer metastasis and prognosis. *J Exp Clin Cancer Res* 2010; **29:** 16.
12. Wilson JL, Burchell J, Grimshaw MJ. Endothelins induce CCR7 expression by breast tumor cells via endothelin receptor A and hypoxia-inducible factor-1. *Cancer Res* 2006; **66:** 11802–11807.
13. Weitzenfeld P, Kossover O, Korner C, *et al*. Chemokine axes in breast cancer: factors of the tumor microenvironment reshape the CCR7-driven metastatic spread of luminal-A breast tumors. *J Leukoc Biol* 2016; **99:** 1009–1025.
14. Pan MR, Hou MF, Chang HC, *et al*. Cyclooxygenase-2 up-regulates CCR7 via EP2/EP4 receptor signaling pathways to enhance lymphatic invasion of breast cancer cells. *J Biol Chem* 2008; **283:** 11155–11163.
15. Cabioglu N, Sahin AA, Morandi P, *et al*. Chemokine receptors in advanced breast cancer: differential expression in metastatic disease sites with diagnostic and therapeutic implications. *Ann Oncol* 2009; **20:** 1013–1019.
16. Kreike B, Hart G, Bartelink H, *et al*. Analysis of breast cancer related gene expression using natural splines and the Cox proportional hazard model to identify prognostic associations. *Breast Cancer Res Treat* 2010; **122:** 711–720.
17. Cabioglu N, Gong Y, Islam R, *et al*. Expression of growth factor and chemokine receptors: new insights in the biology of inflammatory breast cancer. *Ann Oncol* 2007; **18:** 1021–1029.
18. Cassier PA, Treilleux I, Bachelot T, *et al*. Prognostic value of the expression of C-Chemokine Receptor 6 and 7 and their ligands in non-metastatic breast cancer. *BMC Cancer* 2011; **11:** 213.
19. Galea MH, Blamey RW, Elston CE, *et al*. The Nottingham Prognostic Index in primary breast cancer. *Breast Cancer Res Treat* 1992; **22:** 207–219.
20. Abd El-Rehim DM, Pinder SE, Paish CE, *et al*. Expression and co-expression of the members of the epidermal growth factor receptor (EGFR) family in invasive breast carcinoma. *Br J Cancer* 2004; **91:** 1532–1542.
21. Mahmoud SM, Lee AH, Paish EC, *et al*. Tumour-infiltrating macrophages and clinical outcome in breast cancer. *J Clin Pathol* 2012; **65:** 159–163.
22. Mahmoud SM, Paish EC, Powe DG, *et al*. An evaluation of the clinical significance of FOXP3+ infiltrating cells in human breast cancer. *Breast Cancer Res Treat* 2011; **127:** 99–108.
23. Rakha EA, Elsheikh SE, Aleskandarany MA, *et al*. Triple-negative breast cancer: distinguishing between basal and nonbasal subtypes. *Clin Cancer Res* 2009; **15:** 2302–2310.
24. McCarty KS Jr, Miller LS, Cox EB, *et al*. Estrogen receptor analyses. Correlation of biochemical and immunohistochemical methods using monoclonal antireceptor antibodies. *Arch Pathol Lab Med* 1985; **109:** 716–721.
25. Goldhirsch A, Wood WC, Coates AS, *et al*. Strategies for subtypes–dealing with the diversity of breast cancer: highlights of the St. Gallen International Expert Consensus on the Primary Therapy of Early Breast Cancer 2011. *Ann Oncol* 2011; **22:** 1736–1747.
26. Otero C, Groettrup M, Legler DF. Opposite fate of endocytosed CCR7 and its ligands: recycling versus degradation. *J Immunol* 2006; **177:** 2314–2323.
27. Xuan W, Qu Q, Zheng B, *et al*. The chemotaxis of M1 and M2 macrophages is regulated by different chemokines. *J Leukoc Biol* 2015; **97:** 61–69.
28. Zhou S, Shen Z, Wang Y, *et al*. CCR7 expression and intratumoral FOXP3+ regulatory T cells are correlated with overall survival and lymph node metastasis in gastric cancer. *PLoS One* 2013; **8:** e74430.
29. Na IK, Busse A, Scheibenbogen C, *et al*. Identification of truncated chemokine receptor 7 in human colorectal cancer unable to localize to the cell surface and unreactive to external ligands. *Int J Cancer* 2008; **123:** 1565–1572.
30. Schaeuble K, Hauser MA, Rippl AV, *et al*. Ubiquitylation of the chemokine receptor CCR7 enables efficient receptor recycling and cell migration. *J Cell Sci* 2012; **125:** 4463–4474.

SUPPLEMENTARY MATERIAL ONLINE

Supplementary Text. Results of Akaike Information Criterion analysis

Table S1. Statistical associations of total CCR7 cytoplasmic and membrane expression with clinico-pathological parameters

Figure S1. Full face staining of CCR7 in IBC shows homogenous patterns of positivity. Marginal low expression of CCR7 was detected in a few lymphocytes (<1%), red arrows. (**A**) at 4x (**B**) at 10x, (**C**) at 20x, and (**D**) at 40x magnification power